nature structural & molecular biology

SUPPLEMENTARY INFORMATION

https://doi.org/10.1038/s41594-019-0297-8

In the format provided by the authors and unedited.

The molecular mechanism of cotranslational membrane protein recognition and targeting by SecA

Shuai Wang[1,3], Ahmad Jomaa[2,3], Mateusz Jaskolowski[2], Chien-I Yang[1], Nenad Ban[2]* and Shu-ou Shan[1]*

[1]Division of Chemistry and Chemical Engineering, California Institute of Technology, Pasadena, CA, USA. [2]Department of Biology, Institute of Molecular Biology and Biophysics, ETH Zurich, Zurich, Switzerland. [3]These authors contributed equally: S. Wang, A. Jomaa *e-mail: ban@mol.biol.ethz.ch; sshan@caltech.edu

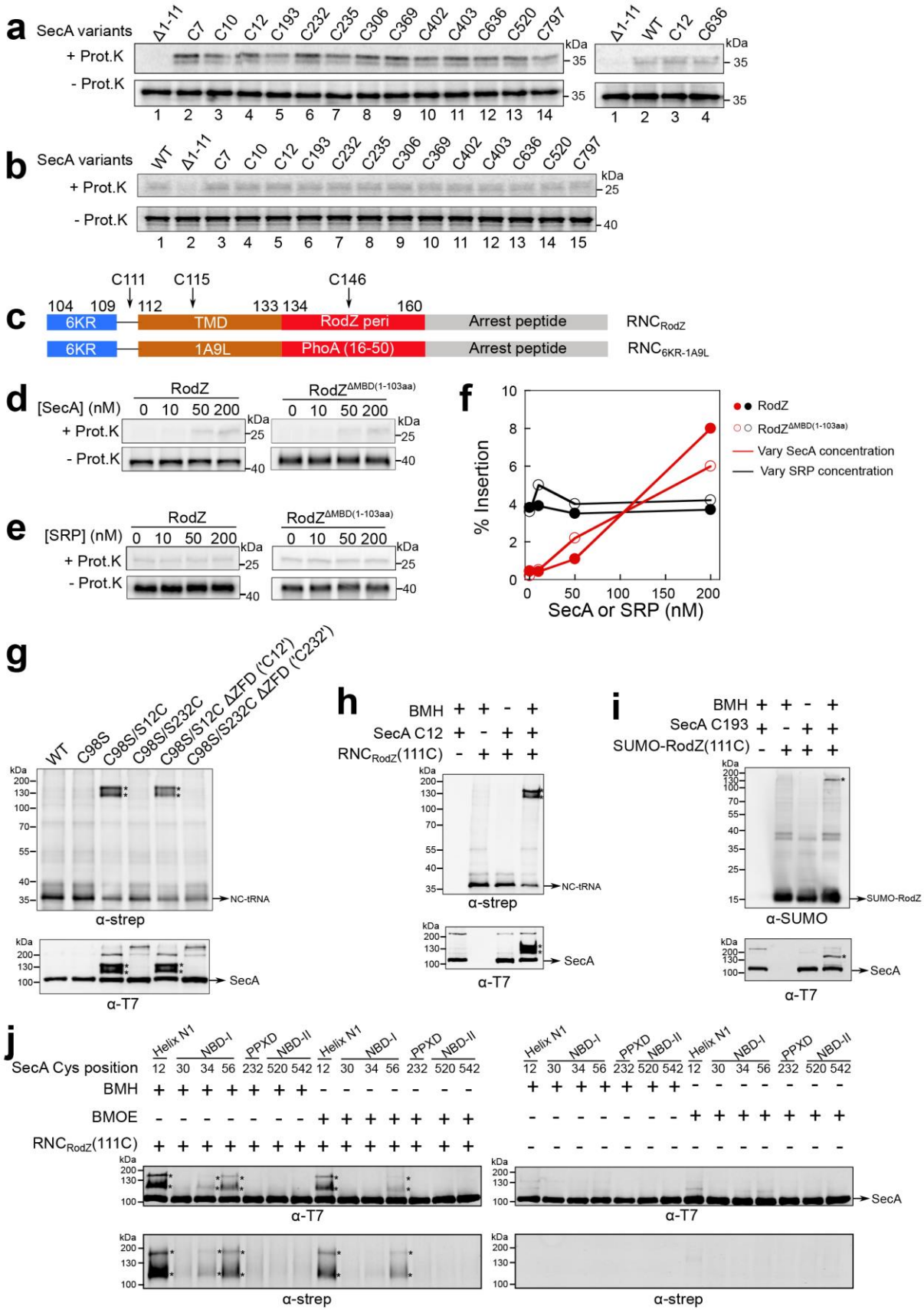
a
SecA variants
Δ1-11 C7 C10 C12 C193 C232 C235 C306 C369 C402 C403 C636 C520 C797
+ Prot.K
- Prot.K
kDa
35
1 2 3 4 5 6 7 8 9 10 11 12 13 14
Δ1-11 WT C12 C636
1 2 3 4
b
SecA variants
WT Δ1-11 C7 C10 C12 C193 C232 C235 C306 C369 C402 C403 C636 C520 C797
+ Prot.K
- Prot.K
kDa
25
40
1 2 3 4 5 6 7 8 9 10 11 12 13 14 15
c
C111 C115 C146
104 109 112 133 134 160
6KR
TMD
RodZ peri
Arrest peptide
RNC_RodZ
6KR
1A9L
PhoA (16-50)
Arrest peptide
RNC_6KR-1A9L
d
[SecA] (nM)
RodZ
RodZ^ΔMBD(1-103aa)
0 10 50 200
+ Prot.K
- Prot.K
kDa
25
40
e
[SRP] (nM)
RodZ
RodZ^ΔMBD(1-103aa)
0 10 50 200
+ Prot.K
- Prot.K
kDa
25
40
f
% Insertion
SecA or SRP (nM)
0 50 100 150 200
0 2 4 6 8 10
RodZ
RodZ^ΔMBD(1-103aa)
Vary SecA concentration
Vary SRP concentration
g
WT C98S C98S/S12C C98S/S232C C98S/S12C ΔZFD ('C12') C98S/S232C ΔZFD ('C232')
kDa
200 130 100 70 55 40 35
NC-tRNA
α-strep
kDa
200 130 100
SecA
α-T7
h
BMH + + - +
SecA C12 + - + +
RNC_RodZ(111C) - + + +
kDa
200 130 100 70 55 40 35
NC-tRNA
α-strep
kDa
200 130 100
SecA
α-T7
i
BMH + + - +
SecA C193 + - + +
SUMO-RodZ(111C) - + + +
kDa
200 130 100 70 55 40 35 25 15
SUMO-RodZ
α-SUMO
kDa
200 130 100
SecA
α-T7
j
Helix N1 NBD-I PPXD NBD-II Helix N1 NBD-I PPXD NBD-II
SecA Cys position
12 30 34 56 232 520 542 12 30 34 56 232 520 542
BMH + + + + + + + - - - - - - -
BMOE - - - - - - - + + + + + + +
RNC_RodZ(111C) + + + + + + + + + + + + + +
kDa
200 130 100
α-T7
α-strep
SecA
α-T7
α-strep

Supplementary Figure 1

Controls and additional data to map the interaction of SecA with hydrophobic sequences on nascent protein in the co- versus post-translational mode.

a-b, The activity of SecA variants were tested by assaying the translocation of proOmpA, a model post-translational SecA substrate (a), and RodZ, a model co-translational SecA substrate (b). ProOmpA and RodZ was in vitro translated using the PURE system supplemented with 1 μM SecA variants and urea-washed inverted membrane vesicles as described previously (Wang, S. et al., *J Cell Biol*. 216, 3639-3653, 2017). Successful insertion into the membrane was detected by protection against proteinase K (Prot.K) digestion. In the left panel of part (a), lane 1 shows the reaction of mutant SecA with deletion on residues 1-11, and lanes 2-14 show the data with single cysteine variants of SecA. The right panel of part (a) shows the comparison of representative single cysteine mutants of SecA relative to wild type (WT) SecA. The data in each gel are from side-by-side experiments.

c, Scheme of the composition of the nascent chains on stalled RNCs used in this study. MreB-binding domain (MBD, residues 1-103) was removed from the RodZ nascent chain. Arrest peptide is from SecM residues 133-170. The positions of engineered cysteines at residues 111, 115 and 146 are indicated. 1A9L nascent chain was constructed by replacing the TMD of RodZ with 1A9L (Jomaa, A. et al., *Nat Commun*. 7, 10471, 2016) followed by the mature region (residues 16-50) of PhoA. RNC, ribosome-nascent chain complex.

d-f, The Mreb-binding domain (MBD; residues 1-103) of RodZ is not essential for SecA-dependent co-translational translocation in a coupled in vitro translation-translocation assay. As previously described (Wang, S. et al., *J Cell Biol*. 216, 3639-3653, 2017), RodZ or $RodZ^{\Delta MBD}$ was translated using the PURE system supplemented with the indicated concentrations of SecA (d) or SRP (e) and urea-washed, inverted membrane vesicles. Successful insertion into the membrane was detected by protection against proteinase K (Prot.K) digestion. The reactions in (d) also contained 3.8 μM trigger factor, 400 nM SRP, 1 μM FtsY. The reactions in (e) also contained 3.8 μM trigger factor, 50 nM SecA, and a fivefold excess of FtsY over SRP. (f) Summary of the insertion efficiency of RodZ or $RodZ^{\Delta MBD}$ from the data in (d) and (e). Insertion efficiency was calculated by dividing the amount of proteinase K-resistant protein by the total amount of protein, normalized by the number of methionines before and after Prot.K digestion.

g, Crosslinking of SecA to C111 in the RodZ nascent chain depends on engineered cysteine on SecA. All lanes contain the BMH crosslinker. Wild type (WT) SecA contains four cysteines (residue 98, 885, 887, 896), none of which crosslinked to RodZ nascent chain. In C98S, the cysteine at residue 98 was mutated to serine. In ΔZFD, the non-essential C-terminus of SecA containing three cysteines were removed. All the other crosslinking experiments in this work contained the C98S mutation and ΔZFD deletion for clean interpretation of results. Asterisks indicate crosslinked products detected by the anti-strep and anti-T7 antibodies.

h, Crosslinking of SecA(C12) to C111 in the RodZ nascent chain depends on the crosslinker, SecA and RNC_{RodZ}. Asterisks indicate crosslinked products detected by the anti-strep and anti-T7 antibodies.

i, Crosslinking of SecA (C193) to C111 in SUMO-RodZ depends on the crosslinker, SecA and SUMO-RodZ. Asterisks indicate crosslinked products detected by the anti-SUMO and anti-T7 antibodies.

j, Engineered single cysteines at the indicated positions of SecA were tested for crosslinking to RodZ (C111) on RNC by BMH or BMOE. Asterisks indicate crosslinked products that are detected by the anti-strep and anti-T7 antibodies.

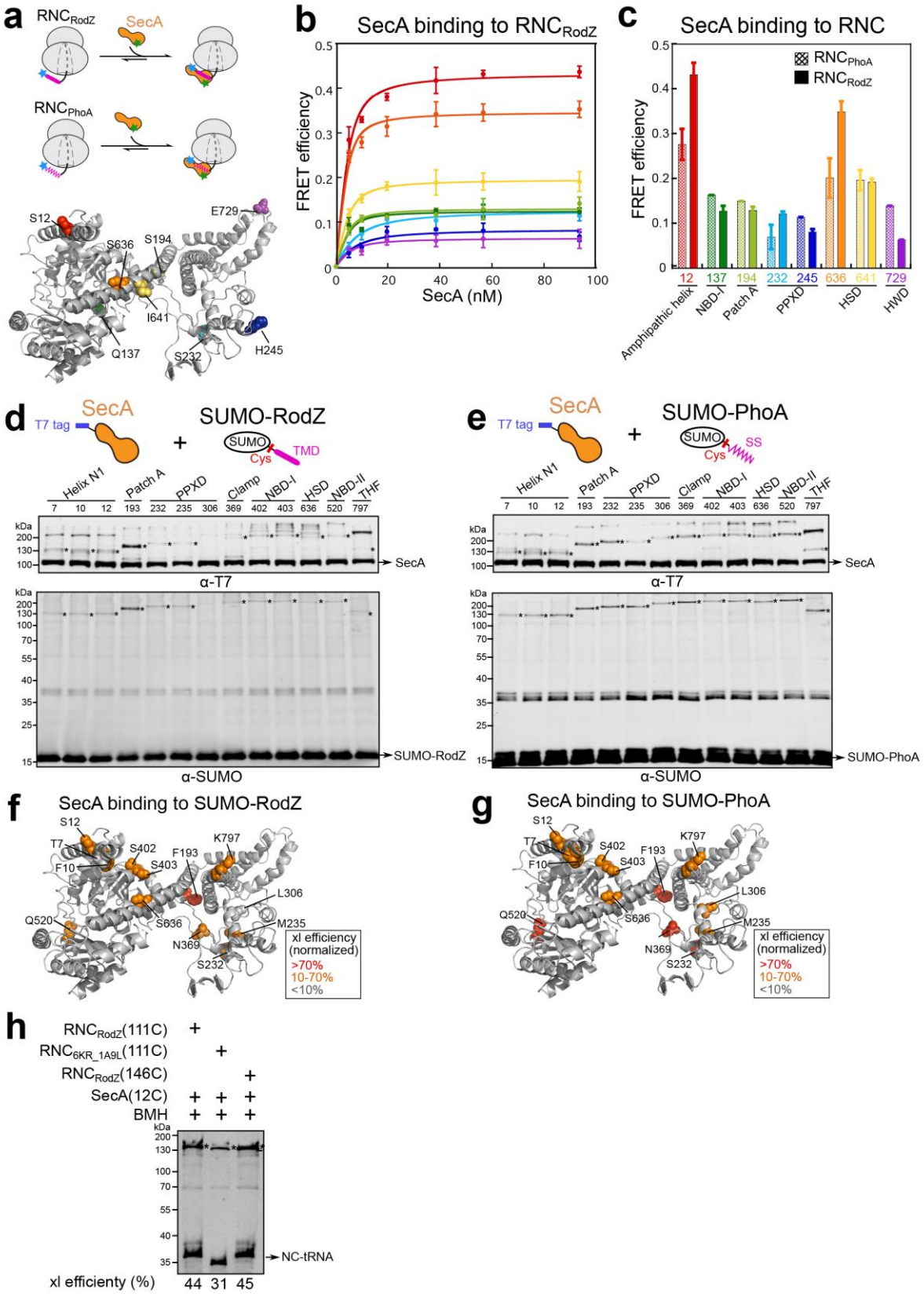

Supplementary Figure 2

Additional data to map the interaction surface of SecA with nascent chains on RNC and with post-translational substrates.

a, FRET experiments to monitor the proximity between Cm (blue star)-labeled RNC_{RodZ} or RNC_{phoA} and BDP (green star) labeled at indicated positions on SecA. Cm was incorporated at residue 111 immediately upstream of the RodZ TMD (magenta) or residue 4 upstream of the phoA signal sequence (magenta). Top left panel, scheme of the FRET-based binding assay. Lower left panel, SecA residues for acceptor labeling are mapped onto the structure of SecA from this work.

b, Representative equilibrium titrations showing the binding of $SecA^{BDP}$ to Cm-labeled RNC_{RodZ}. Reactions used 20 nM RNC^{Cm} (donor) and indicated concentrations of $SecA^{BDP}$ (acceptor). All titrations saturated above 20 nM SecA, indicating tight binding of all the fluorescently labeled SecA variants. The data for individual SecA variants are colored as in the lower panel of (a).

c, Summary of FRET efficiency in the complexes formed between the indicated SecA variants and RNC_{RodZ} or RNC_{PhoA}. FRET efficiency was calculated at 500 nM $SecA^{BDP}$ according to Eq. 1 (Supplementary Note 1). The data for individual SecA positions are colored as in the lower panel of (a). All values represent mean ± s.d., with n = 2-3 independent experiments.

d-e, Engineered single cysteines at indicated positions on SecA were tested for crosslinking by BMH to the RodZ TMD (residues 104-133) or the phoA signal sequence (residues 1-21) fused to the C-terminus of SUMO (SMT3 residues 1-101). The cysteines on RodZ and PhoA are at the same locations as in Fig. 1a and b, respectively. Crosslinking reactions used 8.3 μM SUMO fusion proteins and 1 μM SecA. Asterisks denote crosslinked products detected by both the anti-SUMO and anti-T7 antibodies.

f-g, Crosslinking efficiency from the data in parts (d) and (e), respectively, are summarized in the structural model of SecA from this work. Crosslinking efficiencies (normalized) were relative to the crosslinked product formed by SecA (C193), based on western-blots against SUMO and strep-tag. Residues are colored based on crosslinking efficiency as indicated.

h, Characterization of samples for cryoEM. RNCs were tested for crosslinking between the indicated cysteines on the nascent chain and SecA (C12). RNC_{6KR_1A9L} contained a model signal sequence 1A9L in place of the RodZ-TMD preceded by six consecutive basic residues derived from residues 104-109 of RodZ. Single bands were observed for both the tRNA-linked nascent chain and crosslinked products with SecA, probably due to the removal of polysomes during preparation of the samples for cryoEM. Asterisks denote major crosslinked products detected by anti-strep antibody. Crosslinking efficiency was quantified from the ratio of the intensity of crosslinked nascent chain relative to the total intensity of bands containing the nascent chain.

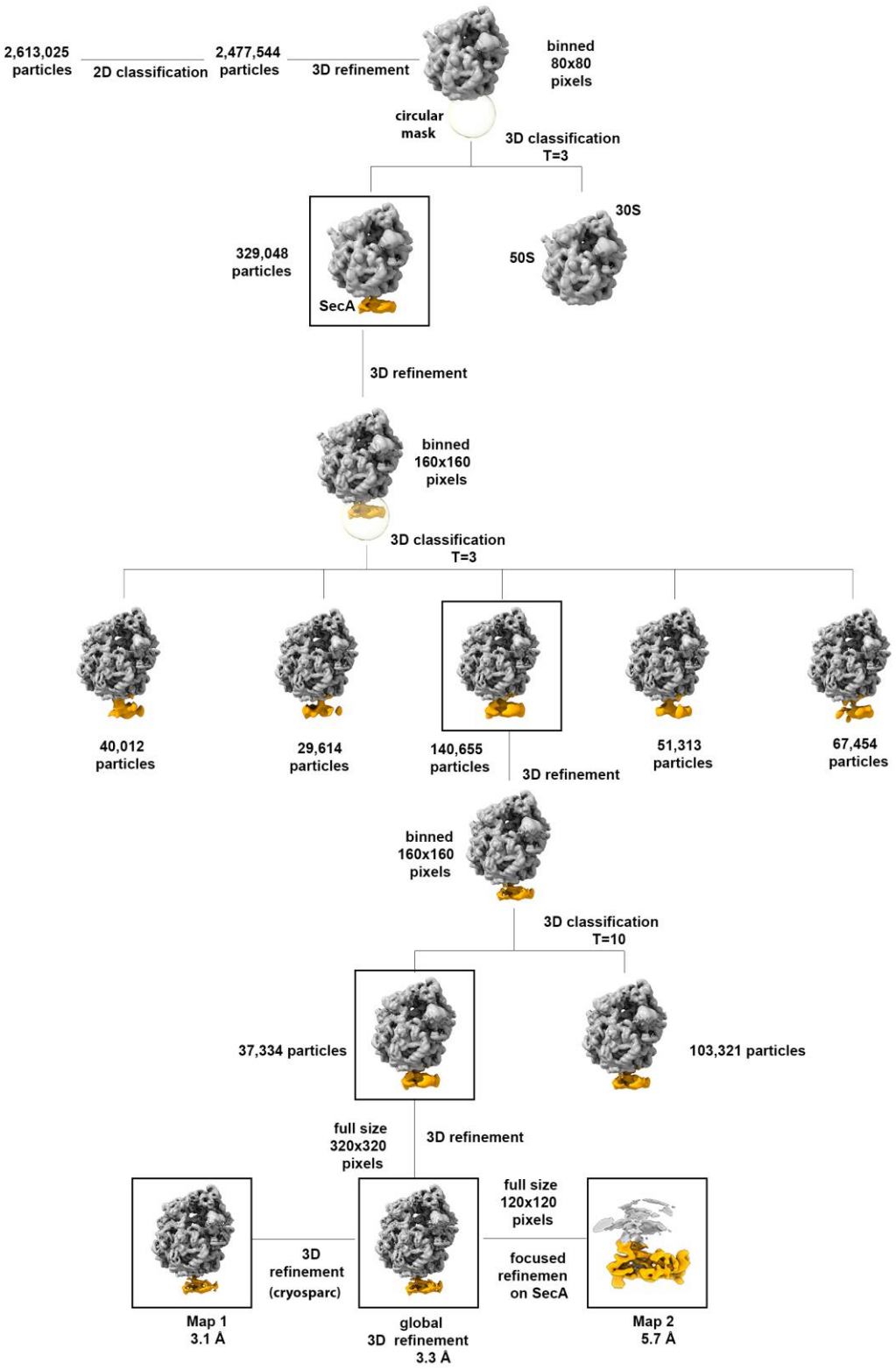

Supplementary Figure 3

Image classification and refinement of the structure of the RNC_{RodZ}•SecA complex.

An initial 2D classification was performed on 4-fold binned particles with pixel size of 5.56 Å per pixel (box size 80 x 80 pixels) to remove bad particles. The selected particle images were then subjected to 3D refinement in RELION3 to obtain an initial map of the ribosome. Using a circular mask applied at the ribosome tunnel region, a 3D focused classification without alignment was performed. This approach yielded a 3D class with a density corresponding to SecA. The remaining classes contained either no or weak density at the exit tunnel region and were discarded. A second round of focused 3D classification on two-fold binned images (160 x160 pixels) yielded a class with an improved EM density of SecA. A final round of focused 3D classification by adjusting tau values in RELION3 (T=10), which yielded a 3D class with resolved secondary structure elements in the EM density of SecA. The selected particle images in this 3D class were subjected to a 3D refinement using full size images without binning (320 x 320 pixels) in RELION3, which yielded a map with an overall resolution of 3.3 Å, and was further improved to 3.1 Å when refined in cryoSPARC (Map1). To improve the local resolution of SecA, a focused 3D refinement scheme was used by first shifting the center of the box from the ribosome to SecA and re-extracting the new particle coordinates using the re-centering option in RELION3 (box size 120 x 120 pixels). Local searches along with a mask around the SecA density were then applied, which resulted in a map of SecA resolved to 5.7 Å resolution (Map2).

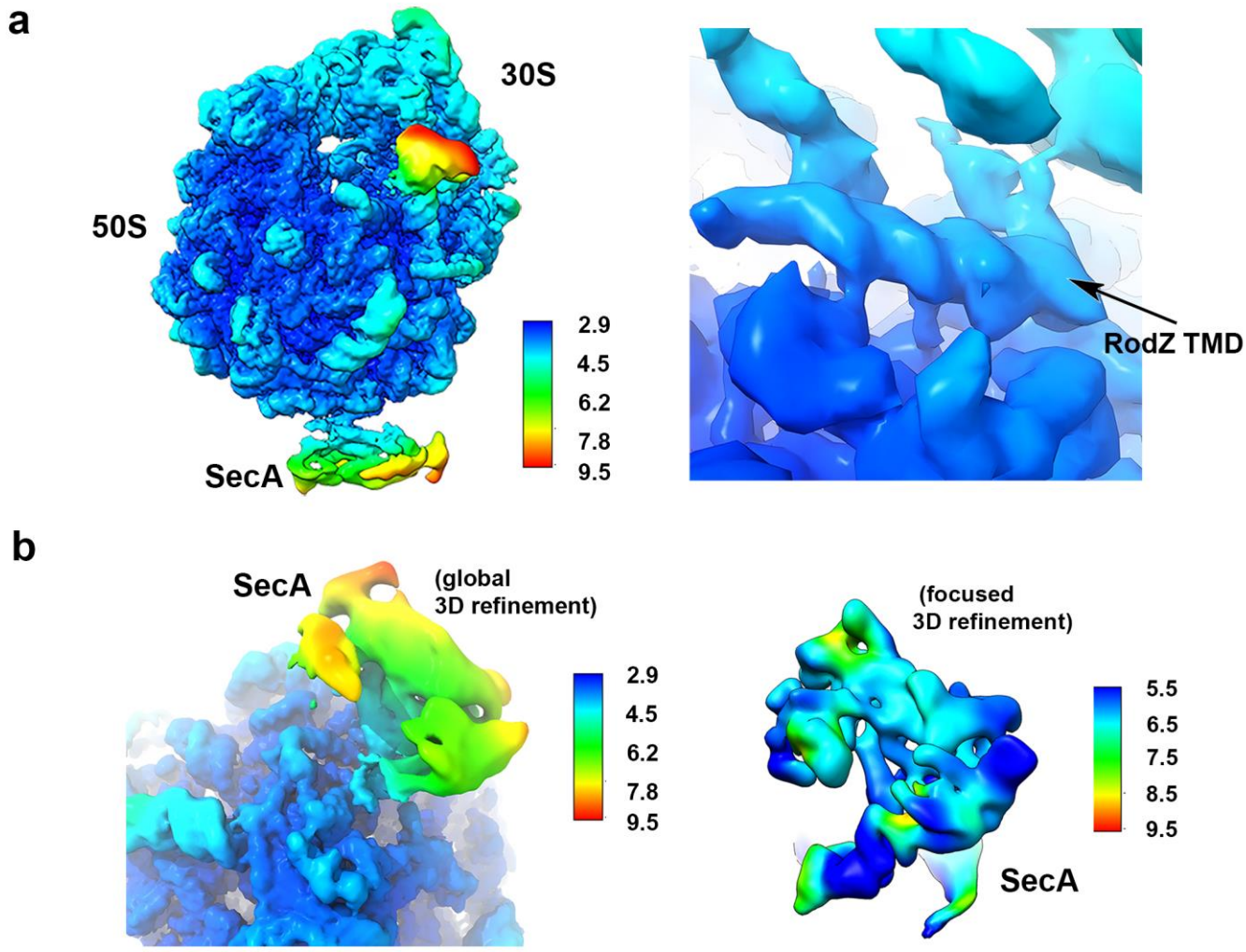
a
30S
50S
SecA
2.9
4.5
6.2
7.8
9.5
RodZ TMD
b
SecA
(global
3D refinement)
2.9
4.5
6.2
7.8
9.5
(focused
3D refinement)
5.5
6.5
7.5
8.5
9.5
SecA
c
Fourier shell correlation
1.0
0.8
0.6
0.4
0.2
FSC=0.5
3.3 Å
5.7 Å
FSC=0.143
3.1 Å
0
0.05
0.1
0.15
0.2
0.25
0.3
0.35
Resolution (1/Å)

Supplementary Figure 4

Local resolution and validation of the cryoEM maps.

a, Local resolution of Map1 obtained from the 3D refinement (left panel), and close-up of the contact points and the resolved density for the RodZ TMD at a similar resolution as the overall resolution (right panel).

b, Comparison of the local resolution plot for the EM density corresponding to SecA using the global refinement approach (left panel) and the focused refinement approach (right panel). Corresponding color keys are shown on the right side of each map.

c, Fourier Shell Correlation (FSC) plots for Map1 (3.1 Å) and Map2 (5.7 Å) using the gold standard FSC criteria cutoff (FSC=0.143) using independent two half maps as implemented in RELION3 and cryoSPARC. Map1 versus obtained model plot shown in red and depicts a similar resolution 3.3 Å using cutoff (FSC=0.5) as that of the cryoEM Map1.

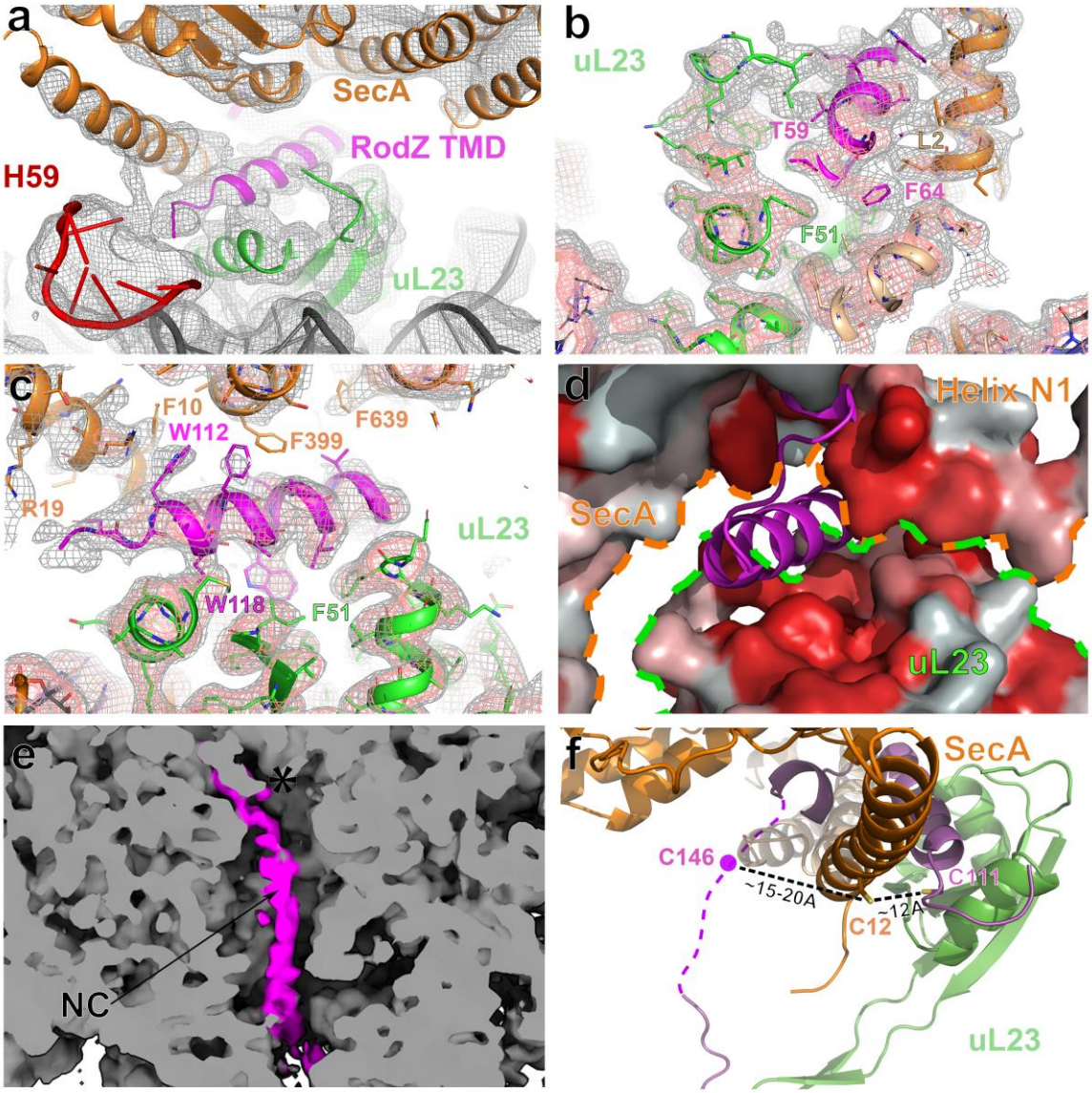

Supplementary Figure 5

Overview of the RodZ TMD binding pocket and the ribosome tunnel region.

a, Close-up of the N-terminal amphipathic helix of SecA in the RNC_{RodZ}•SecA complex with an overlay of the EM-density. Color scheme is the same as in Fig. 3. The EM density was filtered based on the local resolution.

b-c, Local EM-densities outlining regions of RodZ TMD interactions with SecA, uL23, and uL29 are shown with fitted atomic models. EM-densities are low-pass filtered to 3.5 Å resolution for clarity.

d, Hydrophobicity gradient of the TMD binding pocket formed by SecA and uL23. Hydrophobic gradient shows hydrophobic amino acids in red and non-hydrophobic residues to white, applied from script “color_h” in pymol. Orange and green dashed lines outline the surfaces from SecA and uL23,respectively.

e, A cross-section of the ribosome tunnel region with the EM-density of the RodZ nascent chain colored in magenta. The asterisk indicates the position of the CAA end of the P-site tRNA. EM-densities of the RodZ nascent chain was filtered to 4.5 Å resolution for clarity.

f, Distance between C12 of SecA and C111/C146 on the RodZ nascent chain. C12 and C111 are shown in sticks, and the hypothetical location of C146 is shown in sphere. Residues 134-160 of nascent chain are not resolved and are shown as a dashed line.

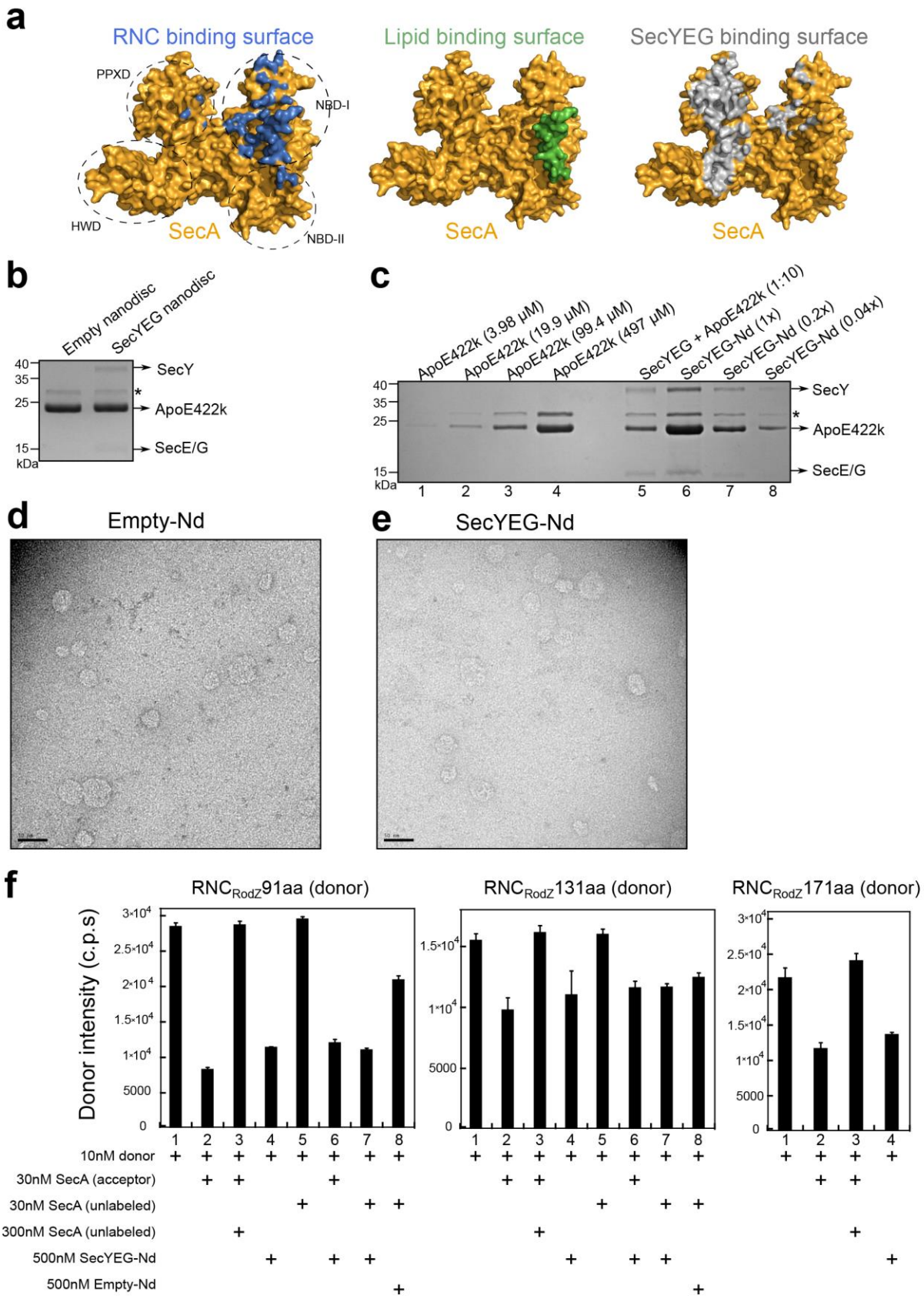
a
RNC binding surface
Lipid binding surface
SecYEG binding surface
PPXD
NBD-I
HWD
NBD-II
SecA
SecA
SecA
b
Empty nanodisc
SecYEG nanodisc
40
35
25
15
kDa
SecY
*
ApoE422k
SecE/G
c
ApoE422k (3.98 μM)
ApoE422k (19.9 μM)
ApoE422k (99.4 μM)
ApoE422k (497 μM)
SecYEG + ApoE422k (1:10)
SecYEG-Nd (1x)
SecYEG-Nd (0.2x)
SecYEG-Nd (0.04x)
40
35
25
15
kDa
SecY
*
ApoE422k
SecE/G
1 2 3 4 5 6 7 8
d
Empty-Nd
e
SecYEG-Nd
f
RNCRodZ91aa (donor)
RNCRodZ131aa (donor)
RNCRodZ171aa (donor)
Donor intensity (c.p.s)
3×10^4
2.5×10^4
2×10^4
1.5×10^4
1×10^4
5000
0
1 2 3 4 5 6 7 8
1 2 3 4
10nM donor
30nM SecA (acceptor)
30nM SecA (unlabeled)
300nM SecA (unlabeled)
500nM SecYEG-Nd
500nM Empty-Nd

Supplementary Figure 6

Characterization of the samples for fluorescence measurements of RNC_{RodZ} transfer from SecA to SecYEG.

a, SecA surfaces contacting RNC (blue), anionic phospholipid (green), and SecYEG (grey). Blue and grey highlight SecA residues within 6 Å of RNC (this work) and SecYEG (PDB ID 5EUL), respectively. Green highlights residues 1-20 of SecA that mediate its lipid binding (Koch, S. *et al*., *J Biol Chem* **291**, 22534-22543, 2016).

b, Coomassie-blue stained gel showing reconstituted ApoE422k nanodisc (Nd) with and without SecYEG. ApoE422k contains two thrombin cleavage sites at the N-terminus, and the observed minor band (asterisk, ~5% of total) may represent incompletely cleaved ApoE422k.

c, Quantification of SecYEG-Nd by Coomassie-blue stained gel. Lanes 1-4 are purified ApoE422k at known concentrations. Lanes 6-8 are reconstituted SecYEG-Nd at different dilutions. Lane 5 shows the mixture of SecYEG:ApoE422k:lipid (molar ratio = 0.1:1:91) before removing detergent (see methods). The intensity of bands with purified ApoE422k was used to generate a standard curve from which we calculated the concentration of ApoE422k in the nanodisc. The concentration of nanodisc was determined to be 136.5 μM by dividing the concentration of ApoE422k in nanodisc by 8 (see Method). The concentration of SecYEG in nanodisc was 75.4 μM, determined as with ApoE422k using purified SecYEG to construct a standard curve. These values indicate that there is 0.55 copy of SecYEG per copy of nanodisc on average.The observed minor band (asterisk, ~5% of total) may represent incompletely cleaved ApoE422k.

d-e, Negative stain electron microscopy images of the empty (d) and SecYEG (e) nanodiscs. Scale bar: 50 nm.

f, Summary of the steady-state fluorescence intensity of the Cm dye on RNC_{RodZ} under the indicated reactions. RNC_{RodZ} 91aa, 131aa, and 171aa contains RodZ residues 104-160, 104-200, and 104-240, respectively. Nd, nanodisc. c.p.s, counts per second.

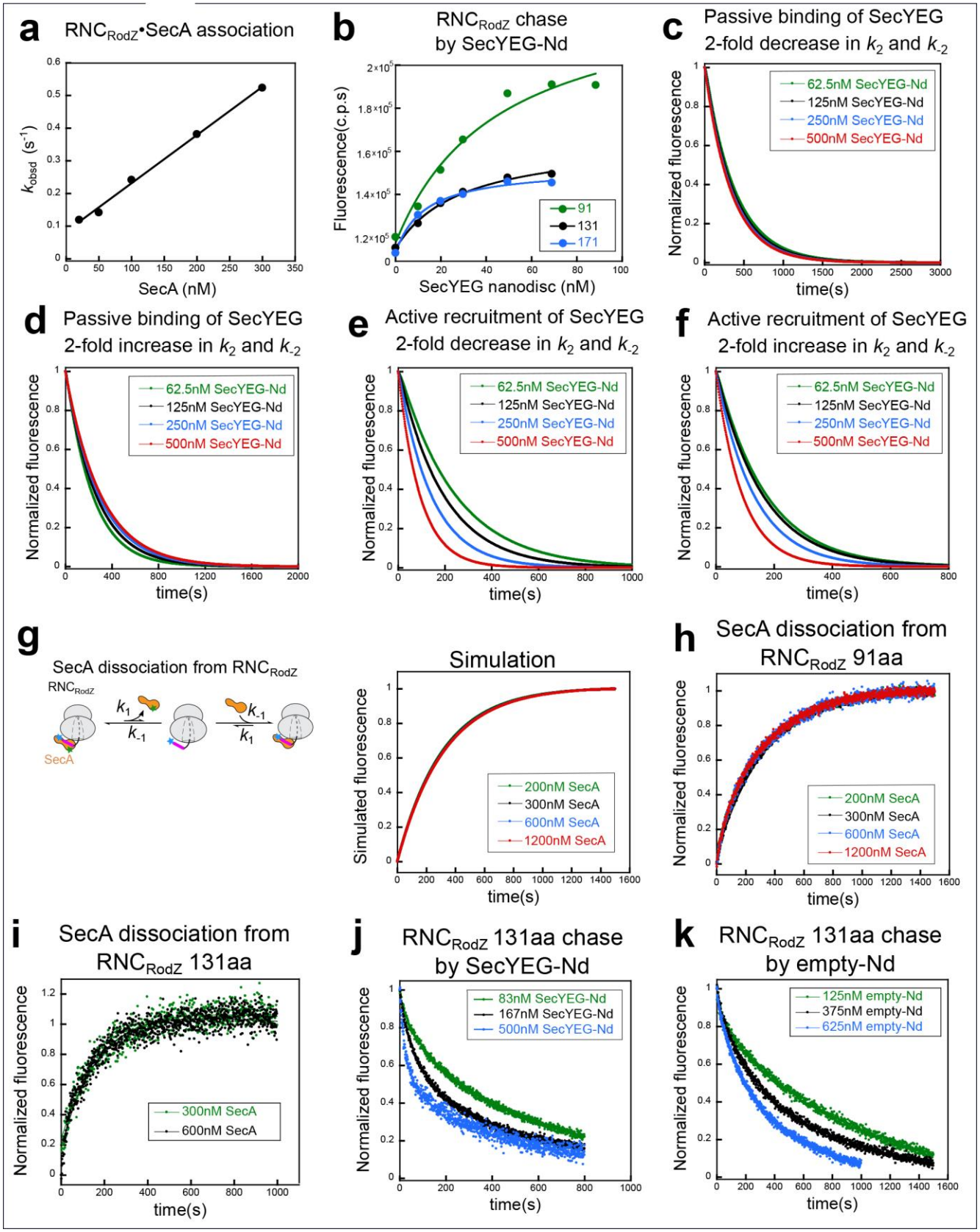

Supplementary Figure 7

Supporting information for the kinetic simulations, and additional data for chase experiments of the RNC_{RodZ}•SecA complex.

a, Measurement of the association rate constant of the SecA•RNC_{RodZ} complex. 10 nM Cm-labeled RNC_{RodZ} was mixed with indicated concentrations of BDP-labeled SecA, and the fluorescence change was fit to Eq. 3 (Supplementary Note 1) to extract the observed association rate constant (k_{obsd}). The value of k_{obsd} was plotted against SecA concentration and fit to Eq. 7 (Supplementary Note 1) to determine k_{-1}.

b, Equilibrium measurement of the transfer reaction. 10 nM at indicated chain lengths was pre-incubated with 30 nM BDP-labeled SecA. Increasing amounts of SecYEG-Nd were then added to the preformed complex, and the increase in Cm fluorescence due to the loss of FRET was monitored. The data were fit to Eq. 8 (Supplementary Note 1) and gave a $K_{1/2}$ value of 45 ± 18 nM, 29 ± 5.4 nM, and 13 ± 2.1 nM for RNC_{RodZ} at nascent chain lengths of 91, 131, and 171aa, respectively.

c-f, Changes in the rate constants of RNC_{RodZ}•SecYEG association (k_2) and dissociation (k_{-2}) (the K_d value for RNC_{RodZ}•SecYEG was held constant) do not affect the kinetics behavior for both the passive (c,d) and active (e,f) models.

g, Reaction scheme (left) and simulation (right) of the experiments to measure the dissociation rate constant (k_1) of SecA from RNC_{RodZ}. A preformed complex of Cm (blue star)-labeled RNC_{RodZ} with BDP-labeled SecA was chased with excess unlabeled SecA to initiate complex dissociation, and the loss of FRET was monitored in real time.

h-i, Representative time courses for measurement of k_1 at nascent chain lengths of 91aa (h) and 131aa (i). The data were fit to Eq. 3. All traces are the average of 6-8 measurements.

j-k, Representative fluorescence time traces for chase of SecA-bound RNC_{RodZ} complex with SecYEG-Nd (j) or empty nanodisc (k) at a nascent chain length of 131aa. Reactions were carried out and analyzed as in Fig. 6c,d, and the obtained rate constants are summarized in Fig. 6f. Note that the time traces are biphasic, and control experiment indicated that the slow phase was due to dye bleaching (see Methods).

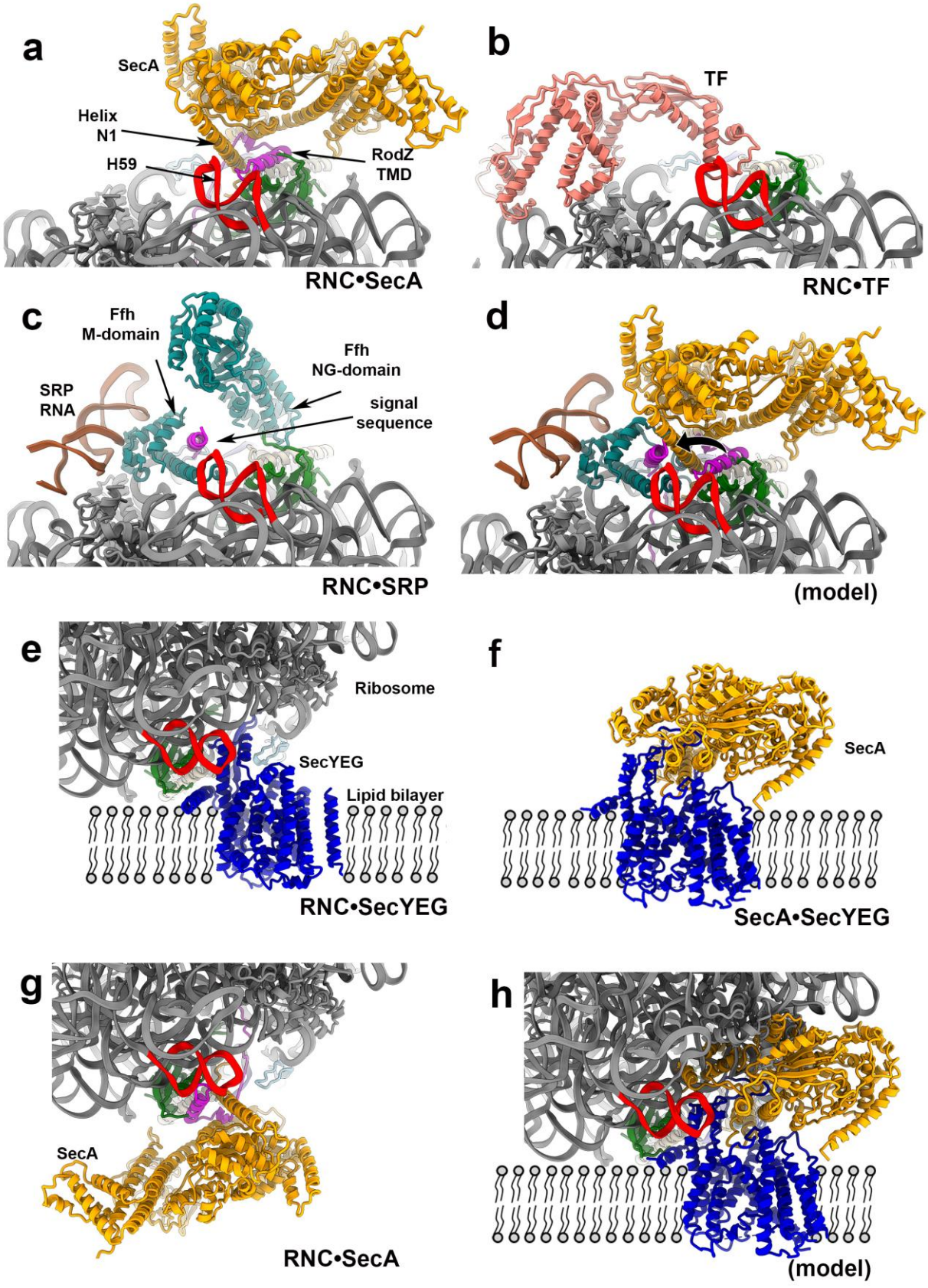
a
SecA
Helix
N1
H59
RodZ
TMD
RNC•SecA
b
TF
RNC•TF
c
Ffh
M-domain
Ffh
NG-domain
SRP
RNA
signal
sequence
RNC•SRP
d
(model)
e
Ribosome
SecYEG
Lipid bilayer
RNC•SecYEG
f
SecA
SecA•SecYEG
g
SecA
RNC•SecA
h
(model)

Supplementary Figure 8

Comparison of the structure from this work with previous structures.

a-c, Comparisons of SecA (a; this work), TF (b; PDB ID: 1W26 and 1W28) and SRP (c; PDB ID: 5GAF) bound to RNC.

d, Overlay of SecA and SRP on the ribosome. The NG domain of the SRP protein Ffh was removed due to steric clash with SecA. The arrow indicates the difference in the position of the signal sequence versus TMD on the ribosome in the presence of SRP versus SecA. The following coloring scheme is used. TF, salmon; Ffh, cyan; SRP RNA, dark orange; signal sequence and TMD, magenta.

e-g, Comparison of the structure of the RNC•SecA complex (g; this work) with the RNC•SecYEG (e; PDB ID: 3J46) and SecA•SecYEG (f; PDB ID: 5EUL) structures. The color scheme is: SecA, orange; SecYEG, blue; uL23, green; H59, red; RodZ TMD, magenta.

h, The structures of SecA- (PDB ID 5EUL) and RNC-bound SecYEG (PDB ID: 3J46) were overlaid to show the steric clash between SecA and RNC on SecYEG.

Supplementary Note 1: Fluorescence measurements and kinetic simulations

Fluorescence measurements

Equilibrium titrations were performed using a Fluorolog-3-22 spectrofluorometer (Jobin Yvon) at room temperature in Assay buffer (50 mM KHEPES, pH 7.5, 150 mM KOAc, 10 mM $Mg(OAc)_2$, 2 mM DTT, 0.1 mg/ml BSA). Unless otherwise specified, experiments used an excitation wavelength of 360 nm and an emission wavelength of 455 nm. The FRET efficiency was calculated based on equation 1:

$$\mathrm{FRET} = 1 - \frac{F_e}{F_0} \qquad (1)$$

in which F_0 is the fluorescence intensity at 455 nm for Cm-labeled RNC alone. F_e is the fluorescence intensity at 455 nm when the Cm-labeled RNC is incubated with saturating amount of BDP-labeled SecA.

Equilibrium titrations used 10 nM Cm-labeled RNC, and indicated concentrations of SecA or SecYEG nanodisc as the titrant. The data were fit to equation 2:

$$\Delta F_{norm} = 1 \times \frac{[\mathrm{RNC}] + [\mathrm{titrant}] + K_d - \sqrt{\left([\mathrm{RNC}] + [\mathrm{titrant}] + K_d\right)^2 - 4 \times [\mathrm{RNC}][\mathrm{titrant}]}}{2 \times [\mathrm{RNC}]} \qquad (2)$$

in which "Normalized fluorescence change" (ΔF_{norm}) was calculated by dividing the observed fluorescence change at each titrant concentration over the fluorescence change at saturating titrant concentration, so that all titration curves start at 0 and plateau at 1, and the curvature of the titration curves directly reflect the K_d value.

Dissociation rate constants of SecA from RNC were measured using a Kintek stopped flow apparatus at room temperature as described previously[1]. 10 nM Cm-labeled RNC and 30 nM BODIPY-FL-labeled SecA were preincubated in Assay buffer, followed by addition of unlabeled SecA at indicated concentrations as the chase to initiate dissociation of the preformed complex. The time course of observed fluorescence (F) was fit to a double exponential function (equation 3):

$$F = F_e + \Delta F_a \times e^{-k_a t} + \Delta F_b \times e^{-k_b t} \qquad (3)$$

in which F_e is the fluorescence when the reaction reaches equilibrium, ΔF_a and k_a are the magnitude and rate constant of the fast phase, and ΔF_b and k_b are the magnitude and rate constant of the slow phase. The magnitude and rate constants of the slow phase are consistent with fluorescence bleaching of the Cm dye determined in parallel measurements. Hence, the first phase was assigned to SecA dissociation from RNC, and k_a represents the dissociation rate constant (k_1). Normalized fluorescence was calculated by dividing the observed fluorescence change at each time point over the fluorescence change when the reaction is complete, so that all the traces start at 0 and plateau at 1.

Measurements of RNC_{RodZ} transfer from SecA to SecYEG-Nd or empty nanodisc were performed using a Kintek stopped flow apparatus at room temperature in Assay buffer supplemented with 0.5 mM AMP-PNP. 10 nM Cm-labeled RNC was preincubated with 30 nM unlabeled SecA followed by addition of SecYEG nanodisc or empty nanodisc at indicated concentrations. The time course of observed fluorescence (F) was fit to Eq. 3, in which k_a represents the apparent rate constant of RNC transfer. Normalized fluorescence was calculated by subtracting the fluorescence at the end of the time course (1500 sec) from the observed fluorescence at each time point and then dividing over the total change in fluorescence over the reaction time course, so that all the traces start at 1 and plateau at 0.

Kinetic simulations

Simulations in Fig. 6a,b, Supplementary Fig. 7c-f were performed using the Berkeley Madonna software.

For the passive model in Fig. 6a and Supplementary Fig. 7c-d, the following reactions were modeled:

$$RNC_{RodZ} \bullet SecA \underset{k_{-1}}{\overset{k_1}{\rightleftharpoons}} RNC_{RodZ} + SecA \quad (4)$$

$$RNC_{RodZ} + SecYEG \underset{k_{-2}}{\overset{k_2}{\rightleftharpoons}} RNC_{RodZ} \bullet SecYEG \quad (5)$$

For the active model in Fig. 6b and Supplementary Fig. 7e-f, the passive pathway (equations 4 and 5) was included in the simulation of the active model for completeness. The following reactions were modeled:

$$RNC_{RodZ} \bullet SecA \underset{k_{-1}}{\overset{k_1}{\rightleftharpoons}} RNC_{RodZ} + SecA \quad (4)$$

$$RNC_{RodZ} + SecYEG \underset{k_{-2}}{\overset{k_2}{\rightleftharpoons}} RNC_{RodZ} \bullet SecYEG \quad (5)$$

$$RNC_{RodZ} \bullet SecA + SecYEG \underset{k_{-3}}{\overset{k_3}{\rightleftharpoons}} RNC_{RodZ} \bullet SecYEG + SecA \quad (6)$$

The initial concentrations of all species were set based on experiment conditions as described under "Fluorescence measurements":

$[RNC_{RodZ}\bullet SecA]_0 = 10$ nM

$[SecA]_0 = 20$ nM

$[RNC_{RodZ}]_0 = 0$ nM

$[RNC_{RodZ}\bullet SecYEG]_0 = 0$ nM

$[SecYEG]_0$: varied concentrations as indicated

The SecA dissociation rate constant, k_1, was experimentally determined for RNC_{RodZ91} (0.00309 s^{-1}, Fig. 5c). To measure the SecA association rate constant (k_{-1}), we monitored the association of RNC_{RodZ} with varying concentrations of SecA using the FRET assay (Supplementary Fig. 7a). The observed rate constant of SecA binding to RNC_{RodZ} (k_{obsd}) was plotted as a function of SecA concentration and fit to equation 7:

$$k_{obsd} = k_{on}[\text{titrant}] + k_{off} \quad (7)$$

in which SecA is the titrant, k_{on} is the SecA association rate constant (k_{-1}) and was determined to be $1.48 \times 10^6\ M^{-1}s^{-1}$. The dissociation constant (K_{d1}) of the $RNC_{RodZ91}\bullet SecA$ complex was calculated to be 2.2 nM ($K_{d1} = k_1/k_{-1}$).

To obtain the dissociation constant (K_{d2}) of the RNC_{RodZ91}•SecYEG formed in the transfer reaction, we titrated SecYEG-Nd during the transfer. We preformed a complex of 10 nM RNC^{Cm}_{RodZ} with 30 nM BDP-labeled SecA, and added increasing amounts of SecYEG-Nd; the increase in Cm fluorescence due to the loss of FRET was used to monitor the transfer reaction (Supplementary Fig. 7b). The data were fit to equation 8:

$$F = F_0 + \left(F_e - F_0\right) \times \frac{[\text{SecYEG}]}{[\text{SecYEG}] + K_{1/2}} \quad (8)$$

in which F is the observed Cm fluorescence, F_0 and F_e are the Cm fluorescence at the beginning and end of the titration, respectively, and $K_{1/2}$ is the concentration of SecYEG-Nd required for 50% complete transfer. $K_{1/2}$ was determined to be 45 nM for RNC_{RodZ91}. At this concentration, we have:

$$[\text{RNC}\cdot\text{SecA}] = [\text{RNC}\cdot\text{SecYEG}] \quad (9)$$

$$[\text{RNC}\cdot\text{SecYEG}] + [\text{SecYEG}] = 45.4\ \text{nM} \quad (10)$$

$$[\text{RNC}\cdot\text{SecA}] + [\text{SecA}] = 30\ \text{nM} \quad (11)$$

$$[\text{RNC}\cdot\text{SecA}] + [\text{RNC}\cdot\text{SecYEG}] + [\text{RNC}] = 10\ \text{nM} \quad (12)$$

$$K_{d1} = \frac{[\text{RNC}]\times[\text{SecA}]}{[\text{RNC}\cdot\text{SecA}]} = 2.2\ \text{nM} \quad (13)$$

$$K_{d2} = \frac{[\text{RNC}]\times[\text{SecYEG}]}{[\text{RNC}\cdot\text{SecYEG}]} \quad (14)$$

$$K_{trans} = \frac{[\text{RNC}\cdot\text{SecYEG}]\times[\text{SecA}]}{[\text{RNC}\cdot\text{SecA}]\times[\text{SecYEG}]} = \frac{K_{d1}}{K_{d2}} = \frac{k_3}{k_{-3}} \quad (15)$$

Solving equations 9-15 gave K_{d2} = 3.4 nM and K_{trans} = 0.62. The association rate constant of RNC_{RodZ} binding to SecYEG (k_2) was assumed to be $1 \times 10^6\ M^{-1}s^{-1}$, which is typical for bi-molecular association. This results in a dissociation rate constant ($k_{-2} = K_{d2} \times k_2$) for the RNC_{RodZ}•SecYEG complex of 0.00338 s^{-1}, which is consistent with the previous observation that the half-life of the RNC•SecYEG complex is ~250 s^2. Varying the values of k_2 and k_{-2} while

maintaining the value of K_{d2} did not affect the outcome of the simulation (Supplementary Fig. 7c-f).

To measure the rate constant k_3, the observed transfer rate of RNC_{RodZ91} in Fig. 6e (green) was fit to equation 7, where $k_3 = k_{on}$ and was determined to be $1.4 \times 10^4\ M^{-1}\ s^{-1}$. k_{-3} was calculated to be $2.3 \times 10^4\ M^{-1}\ s^{-1}$ based on equation 15.

Because the formation of RNC_{RodZ}•SecYEG complex causes fluorescence quenching of RNC_{RodZ}, the simulated fluorescence (F_{sim}) starts at 1 at time = 0s, and is proportional to the sum of the fraction of RNC_{RodZ} and RNC_{RodZ}•SecA complex. Normalized fluorescence was simulated as $(F_{sim}\text{-}F_{sim,e})/(1\text{-}F_{sim,e})$ in which $F_{sim,e}$ is the fraction of F_{sim} when the reaction is complete, so that the traces start at 1 and plateau at 0.

To simulate the pulse-chase experiments to measure SecA dissociation from RNC_{RodZ} in Supplementary Fig. 7g, the following reactions were used:

$$RNC_{RodZ} \bullet SecA_{BDP} \underset{k_{-1}}{\overset{k_1}{\rightleftharpoons}} RNC_{RodZ} + SecA_{BDP} \quad (16)$$

$$RNC_{RodZ} + SecA \underset{k_1}{\overset{k_{-1}}{\rightleftharpoons}} RNC_{RodZ} \bullet SecA \quad (17)$$

In which $SecA_{BDP}$ and SecA denote BODIPY-FL labeled and unlabeled SecA, respectively. The initial concentrations of all species were set based on experiment conditions as described above under “Fluorescence measurements”:

$[RNC_{RodZ}\text{•}SecA_{BDP}]_0 = 10$ nM

$[SecA_{BDP}]_0 = 20$ nM

$[RNC_{RodZ}]_0 = 0$ nM

$[SecA]_0$: varied concentrations as indicated

As described above, k_1 and k_{-1} were set to $0.00309\ s^{-1}$ and $1.48 \times 10^6\ M^{-1}s^{-1}$, respectively. Normalized fluorescence change during the chase is proportional to the fraction of the

RNC_{RodZ}•SecA complex and was simulated as $[RNC_{RodZ}•SecA]/[RNC_{RodZ}•SecA]_e$, in which $[RNC_{RodZ}•SecA]_e$ is the RNC_{RodZ}•SecA concentration when the reaction is complete.

References

1. Rome, M.E., Chio, U.S., Rao, M., Gristick, H. & Shan, S.O. Differential gradients of interaction affinities drive efficient targeting and recycling in the GET pathway. *Proc Natl Acad Sci U S A* **111**, E4929-35 (2014).
2. Wu, Z.C., De Keyzer, J., Kedrov, A. & Driessen, A.J.M. Competitive binding of the SecA ATPase and ribosomes to the SecYEG translocon. *J Biol Chem* **287**, 7885-7895 (2012).

Supplementary Note 2: Discussion of equilibrium titration of the transfer reaction.

Equilibrium titrations of the transfer reaction (Supplementary Fig. 7b) showed that, with 30 nM SecA present, the SecYEG concentration required to reach 50% transfer was 45 nM for RNC_{RodZ91}, yielding an estimated equilibria of the transfer reaction (Fig. 6b, $K_{trans} = k_3/k_{-3}$) of 0.62 (Supplementary Note 1). As thermodynamics is pathway-independent, K_{trams} is also the ratio of the affinities of the RNC_{RodZ}•SecA and RNC_{RodZ}•SecYEG complexes (Eq. 15 under Supplementary Note 1). This predicts that the affinity of the RNC_{RodZ}•SecYEG complex generated by the transfer is similar to that of the RNC_{RodZ}•SecA complex, in the low nanomolar range, which is ~100-fold tighter than the K_d value obtained by direct binding of RNC_{RodZ} to SecYEG-Nd (Fig. 5c). This implies that free RNC_{RodZ} was less competent in engaging SecYEG, possibly due to nonproductive conformations in the relatively long nascent chain, and hence formed a weaker complex with the translocon than that generated during transfer from SecA-bound RNC. If the transfer reaction occurred via the passive mechanism involving free RNC_{RodZ} as an obligatory intermediate (Fig. 6a), it would require ~100-fold higher concentrations of SecYEG-Nd than we observed. These considerations strongly suggest that the observed transfer reactions largely bypass the formation of free RNC_{RodZ} that could be conformationally trapped, and that the active transfer mechanism allowed the generation of an RNC_{RodZ}•SecYEG complex much more stable than that obtained from direct addition of RNC_{RodZ} to SecYEG.